# Slow decay rate of correlations induced by long-range extended Dzyaloshinskii-Moriya interactions

Tanoy Kanti Konar[1], Leela Ganesh Chandra Lakkaraju[1,2,3], Aditi Sen(De)[1]
[1] *Harish-Chandra Research Institute, A CI of Homi Bhabha National Institute, Chhatnag Road, Jhunsi, Allahabad - 211019, India*
[2] *Pitaevskii BEC Center and Department of Physics, University of Trento, Via Sommarive 14, I-38123 Trento, Italy and*
[3] *INFN-TIFPA, Trento Institute for Fundamental Physics and Applications, Trento, Italy*

We examine the impact of long-range Dzyaloshinskii-Moriya (DM) interaction in the extended $XY$ model on the phase diagram as well as the static and dynamical properties of quantum and classical correlation functions. It is known that in the nearest-neighbor $XY$ model with DM interaction, the transition from the gapless chiral phase to a gapped one occurs when the strengths of the DM interaction and anisotropy coincide. We exhibit that the critical line gets modified with the range of interactions which decay according to power-law. Specifically, instead of being gapless in the presence of a strong DM interaction, a gapped region emerges which grows with the increase of the moderate fall-off rate (quasi-long range regime) in the presence of a transverse magnetic field. The gapless chiral phase can also be separated from a gapped one by the decay patterns of quantum mutual information and classical correlation with distant sites of the ground state which are independent of the fall-off rate in the gapless zone. We observe that the corresponding critical lines that depend on the fall-off rate can also be determined from the effective central charge involved in the scaling of entanglement entropy. We illustrate that in a non-equilibrium setting, the relaxation dynamics of classical correlation, the decay rate of total correlation, and the growth rate of entanglement entropy can be employed to uncover whether the evolving Hamiltonian and the Hamiltonian corresponding to the initial state are gapped or gapless.



## I. INTRODUCTION

Long-range order across quantum systems is desirable for a variety of quantum technological tasks, as it facilitates the sharing of correlation among distant parts of the system. Historically, such long-range order has been observed in many-body systems at quantum criticality or when the spectrum becomes gapless. In the case of the nearest-neighbor (NN) $XY$ model with nonvanishing anisotropy parameter, it has been demonstrated that the classical correlations decay with the distance between the spins exponentially (polynomially) when it is away from (at) the criticality. Beyond NN models, long-range interacting (LR) systems with power-law decay in the range of interactions have been shown to exhibit polynomial decay of correlations, even when the spectrum is not gapless. These systems become an intense topic of research in the last few years, especially in the context of building analog quantum simulator[1–6] and due to their natural occurrence in several physical platforms such as the Rydberg atom arrays [7], dipolar systems [8], polar molecules [9], trapped-ion setups [10–12], and cold atoms in cavities [13, 14]. Moreover, several established results that hold for nearest-neighbor systems came into the light of investigation in these LR systems in terms of Lieb-Robinson bound [15], area law [16], novel phases of matter [17], dynamical phases [18] and from the perspectives of usefulness in quantum technologies like quantum metrology [19] and quantum computation [20].

The nearest-neighbor Dzyaloshinskii-Moriya (DM) interaction, on the other hand, involves an asymmetric exchange of spins caused by spin-orbit coupling [21–23]. It has been widely explored in a variety of solid-state compounds, including $Cu(C_6D_5COO)_2.3D_2O$ [24, 25], $Yb_4As_3$[26, 27], $CrI_3$ [28] etc, exhibiting fascinating magnetic properties, like gapless chiral phase when the DM interaction strength is stronger than the anisotropy parameter in the transverse Ising [29, 30], $XY$ [31–33] and the gamma model [34]. It was also shown that the DM interaction can host a ground state in the gapless phase that contains logarithmic entanglement behavior, similar to the LR interacting systems which can enhance the fidelity in quantum teleportation [35], thermal entanglement [32, 36–38] and performance in quantum engines [39, 40]. In the non-equilibrium domain, the DM interaction has also been examined in the context of non-equilibrium thermodynamics [41], dynamical quantum phase transitions [42], topological phase transition [43] and quantum speed limit [44].

In this paper, we explore the long-range extended $XY$ model in the presence of long-range extended DM interactions, which decay according to a power-law. Specifically, we aim to analyze the responses of both long-range and DM interactions in equilibrium and non-equilibrium physics. In the former scenario, we present the phase-classification utilizing conventional order parameters, the law for the decreasing slopes of classical and quantum correlations, and the scaling of entanglement entropy (EE) with the corresponding central charge. In contrast to the NN model [32], we show that given a fixed fall-off rates, there exists a gapped region in which the DM interaction is stronger than the anisotropy parameter. However, we establish that whenever the system is gapless, it is chiral. Notably, in the static case, when the ground state belongs to the chiral gapless region, the classical correlation and quantum mutual information decay with constant decreasing exponent while this is not the case in the gapped regime. In this model, we observe that the effective central charge associated with EE exhibits interesting behaviors: in the presence of LR and DM interactions, the central charge acts nonlinearly with multiple kinks that are absent from the extended Ising model without DM interactions.

In comparison to the equilibrium scenario, the dynamical phases could not be efficiently characterized as they depend on the initial state, evolving operator, time and system parameters. In order to distinguish between the gapless and gapped phases, we resort to a recently proposed relaxation dynamics of two-point classical correlations [45–48] and entanglement entropy of the evolved state in the transient regimes, as well

as mutual information and classical correlation in the steady state domains (cf. [49–56] for other dynamical quantities). In our case, the initial state is prepared by tuning the parameters of the Hamiltonian which have either gapless or gapped energy spectra while evolution happens when the range of interactions is suddenly quenched, resulting in a gapless or gapped Hamiltonian. Specifically, in the transient regime, we show that the long-range DM interactions modify the exponent in the relaxation time of the two-point classical correlation between modes and establish a generic scaling law for the growth of entanglement entropy over time. Further, we observe that the behavior of mutual information and classical correlation between two arbitrary sites in the steady state differs depending on whether the Hamiltonians corresponding to the initial and dynamical states are in the same (gapped or gapless) phase or in different phases.

The paper is organized as follows. In Sec. II, we introduce the long-range extended $XY$ model with an additional long-range DM term and find the energy spectra and eigenvectors. While we identify the conventional phases in Sec. II B, we indicate the decay of classical and quantum correlations in Sec. II C. The behavior of entanglement entropy and the corresponding central charge with respect to system parameters are studied in Sec. II D. We then move on to the investigation of features in dynamical states, namely the relaxation dynamics of classical correlations, and the rate of entropy growth in the transient regime in Secs. III and III C respectively while we examine the decay of mutual information with distance between the spins in the steady state in Sec. III B. The results are summarized in Sec. IV.

## II. EMERGENT GAPPED PHASE WITH STRONG DM INTERACTIONS: PHASE DIAGRAM

The critical lines for the long-range interacting $XY$ spin models in the presence of Coloumb-like interaction, described by a parameter $\alpha$ and for the nearest-neighbor transverse $XY$ model with DM interaction are known in the literature [32]. However, the effects of long-range DM interactions has never been addressed before. In this situation, a possible query can be – can the introduction of long-range DM interactions change the critical lines and phases of the LR Ising models? We answer this question affirmatively by first presenting the analytical prescription of this model for obtaining energy spectra and the eigenvectors, thereby leading to the modified phase-portrait of the extended long-range $XY$ model [57, 58] having long-range extended Dzyaloshinskii-Moriya interaction both in the thermodynamic limit and for finite systems. In particular, we report the gapless chiral phase and its dependence on the fall-off rate, $\alpha$. In addition, we identify appropriate order parameters that can reveal $\alpha$-dependence in the modified magentic phase diagram. From the decay patterns of classical correlation including Landau parameters and quantum correlations in terms of quantum mutual information and block entanglement entropy, we again separate the gapless region from the gapped one in this model.

### A. Energy spectrum of the long-range XY and DM interactions

The Hamiltonian, describing long-range extended XY model having long-range extended DM interaction in the presence of transverse magnetic field, reads as

$$H = \sum_{j=1}^{N}\sum_{r=1}^{\frac{N}{2}} -\frac{J'_r}{\mathcal{N}}\Bigg[\frac{1+\gamma}{4}\sigma_j^x\mathbb{Z}_r^z\sigma_{j+r}^x + \frac{1-\gamma}{4}\sigma_j^y\mathbb{Z}_r^z\sigma_{j+r}^y + \frac{D'}{4}(\sigma_j^x\mathbb{Z}_r^z\sigma_{j+r}^y - \sigma_j^y\mathbb{Z}_r^z\sigma_{j+r}^x)\Bigg] - \frac{h'}{2}\sum_{j=1}^{N}\sigma_j^z, \quad (1)$$

where $\mathbb{Z}_r^z = \prod_{l=j+1}^{j+r-1}\sigma_l^z$, with $\mathbb{Z}_1^z = \mathbb{I}$ and $\sigma^k (k = 1, 2, 3)$ is the Pauli matrix, $J'_r = \frac{J}{r^\alpha}$ with $\alpha$ being the strength of power-law decay of the model, $\gamma$ is the anisotropy parameter, $D$ is the strength of the DM interaction, $\mathcal{N} = \sum_{r=1}^{N/2}\frac{1}{r^\alpha}$ is called the Kac-scaling factor [59] which ensures extensivity of the energy in the case of finite-size systems $\alpha < 1$ in the finite-size limit and $h'$ is the strength of the external magnetic field. To make the analysis dimensionless, we redefine the magnetic field as $h = h'/J$ and DM interaction strength as $D = D'/J$. We consider the periodic boundary condition (PBC), i.e., $\sigma_{N+1} \equiv \sigma_1$. This model can be solved analytically by mapping spins into free fermions under the following Jordan-Wigner transformation [60–63]:

$$\begin{aligned}\sigma_n^x &= \left(c_n + c_n^\dagger\right)\prod_{m<n}(1-2c_m^\dagger c_m)\\ \sigma_n^y &= i\left(c_n - c_n^\dagger\right)\prod_{m<n}(1-2c_m^\dagger c_m)\\ \text{and}\quad \sigma_n^z &= 1-2c_n^\dagger c_n, \end{aligned} \quad (2)$$

where $c_m^\dagger(c_m)$ is creation (annihilation) operator of spinless fermions and they follow fermionic commutator algebra. The corresponding free fermionic version of the Hamiltonian takes the form

$$H = \sum_n\sum_r \frac{J_r}{2}\Big((1+iD)c_n^\dagger c_{n+r} + \gamma c_n^\dagger c_{n+r}^\dagger + \text{h.c}\Big) + h(c_n^\dagger c_n - 1/2), \quad (3)$$

where $J_r = \frac{1}{r^\alpha}$. One can observe that the Hamiltonian which is quadratic in fermionic operators have long-range interaction both in hopping and superconducting terms. In addition, an extra hoping term emerges due to the DM interaction which also induces a complex phase. It is worthwhile to mention here that in the absence of DM interaction for $\gamma = 0$, the model is $\mathbb{U}(1)$ symmetric while it is $\mathbb{Z}_2$ symmetric with $\gamma \neq 0$, $D = 0$. The introduction of DM interaction leads to a competition between these two symmetries. In the short-range (SR) models, it is known that the conformal sector changes due to the shift of the symmetry sector [33], responsible for a non-trivial phenomenon.

Due to the presence of translational invariance in the system, momentum is a good quantum number. Hence, we perform a Fourier transform of the form, $c_n = \frac{1}{\sqrt{N}}\sum_k e^{-i\phi_k n}c_k$

where $\phi_k = \frac{\pi(2k-1)}{N}$ $\forall k \in [-N/2, N/2]$ and the corresponding Hamiltonian in the momentum basis can be written as $H = \bigoplus_k H_k$ with

$$\begin{aligned} H_k &= \sum_{k>0} -\Big[\sum_r (\mathrm{Re}(J_k^\alpha) + D\mathrm{Im}(J_k^\alpha))c_k^\dagger c_k \\ &\quad +(\mathrm{Re}(J_k^\alpha) - D\mathrm{Im}(J_k^\alpha))c_{-k}^\dagger c_{-k} \\ &\quad -i\gamma \mathrm{Im}(J_k^\alpha)(c_k^\dagger c_{-k}^\dagger - c_{-k}c_k)\Big] \\ &\quad +h(c_k^\dagger c_k + c_{-k}^\dagger c_{-k}) - h, \end{aligned} \tag{4}$$

and $J_k^\alpha = \sum_{r=1}^{\frac{N}{2}} J_r e^{i\phi_k r}$. This Hamiltonian can be diagonalized by applying the Bogoliubov transformation,

$$\begin{pmatrix} c_k \\ c_{-k}^\dagger \end{pmatrix} = \begin{pmatrix} u_k & -v_k^* \\ v_k & u_k^* \end{pmatrix} \begin{pmatrix} \tau_k \\ \tau_{-k}^\dagger \end{pmatrix}, \tag{5}$$

where $u_k = \cos\theta_k$, $v_k = i\sin\theta_k$ and $\theta_k$ is called Bogoliubov angle, given by $\cos\theta_k = \frac{-h+\mathrm{Re}(J_k^\alpha)-\lambda}{\sqrt{2(\lambda^2-(\mathrm{Re}(J_k^\alpha)-h)^2)}}$ and $\lambda = \sqrt{(h-\mathrm{Re}(J_k^\alpha))^2 + (\gamma\,\mathrm{Im}(J_k^\alpha))^2}$. The eigenvalue corresponding to each momentum, $k$, is given as

$$\epsilon_{\pm k} = -D\,\mathrm{Im}(J_k^\alpha) \pm \lambda. \tag{6}$$

Note first that for $D \neq 0$, although the Bogoliubov basis, $(u_k, v_k)^T$, are independent of DM interactions, $\epsilon_k \neq \epsilon_{-k}$, making the analysis non-trivial. Further, when $D = 0$, this model shows criticality at $h = 1$ and at $h = -1 + 2^{1-\alpha}$ for $\alpha > 1$ corresponding to the both ends of the Brillouin zone, i.e., $\phi_k = 0$ and $\phi_k = \pi$ respectively. In the case of $\alpha < 1$, the energy of the system diverges in the thermodynamic limit, hence, we consider large but finite system size [64]. With the introduction of DM, new gapless region emerges, which changes with $\alpha$ for $D > \gamma$. Such a region is known for the nearest-neighbour $XY$ model when $D > \gamma$ [32] and gapless to gapped transition occurs at $D = \gamma$. However, we now establish that even when $D > \gamma$, long-range interactions can induce a gapped phase instead of a gapless one, which implies the modification of the critical lines in presence of LR interactions.

*Possible experimental implementations of LR model with DM interaction.* Long-range interacting systems occur naturally in trapped-ion experimental platforms, providing a highly regulated set-up for mimicking complicated quantum many-body phenomena [10–12]. Engineering spin-dependent optical dipole forces allows an exact tuning of the interaction range, as defined by the parameter $\alpha$. This tunability enables the investigation of many interaction domains, ranging from practically infinite-range interactions to regimes more akin to short-range behavior. Furthermore, the strength of an effective transverse magnetic field, represented by $h$, can be independently regulated by adjusting the trapping potential in Penning trap configurations. This control is necessary for simulating a variety of quantum magnetic models, including those with quantum phase transitions and critical behaviors [65].

Recent studies have focused on the realization of the Dzyaloshinskii-Moriya interaction, which is quantified by the parameter $D$. According to a recent suggestion [66], a bilayer Penning trap structures may support complex eigenvectors and build effective spin-orbit couplings, making them a feasible way to mimic DM interactions. These studies suggest that a ion-trap experiment in a bilayer Penning trap can effectively simulate DM interaction with the ability to modulate all the parameters such as $\alpha$, $h$ and $D$. Furthermore, there are several trapped ion experiments where long-range Ising interactions have been realized, providing a platform to realize long-range DM interactions [67].

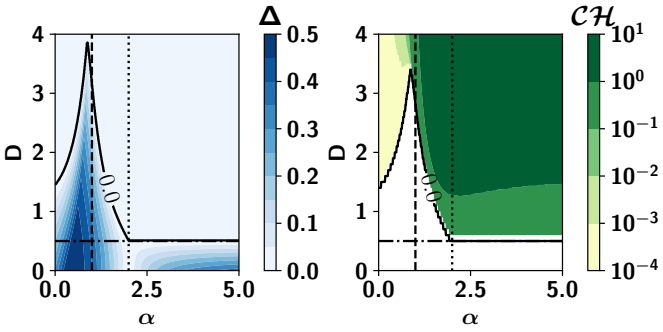


FIG. 1. **Contour plot of $\Delta$ and $\mathcal{CH}$ in the $(\alpha, D)$-plane.** $D$ is the interaction strength of the Dzyaloshinskii-Moriya interaction while $\alpha$ indicates the power-law decay in the range of interactions. Here the anisotropy parameter, $\gamma = 0.5$ and the strength of the magnetic field, $h = -0.5$. For the NN $XY$ model, it is known that the system is gapless when $D > \gamma = 0.5$. However, we find that this is not the case when $1 < \alpha < 2$ and $\alpha < 1$. Moreover, the right-hand sinde figure shows that whenever the system is gapless, it is chiral, i.e., $\mathcal{CH} \neq 0$. The system size is chosen to be $N = 512$. All axes are dimensionless.

Further, it has been suggested that Kitaev chains with long-range hopping and pairing can serve as models for helical Shiba chains, consisting of magnetic impurities in an s-wave superconductor. The introduction of an extended DM interaction results in local phases for this interaction, adding hopping terms that generally involve complex phase factors, which may be simulable in such chains [68]. The experimental signature of the DM interaction is the presence of skyrmions and the chiral nature of magnon quasiparticles. Since the DM interaction arises due to the broken inversion symmetry and strong spin-orbit coupling, it could potentially be realized in spherical FeGe crystals [69].

### B. The gapless chiral phase depending on LR interactions

Apart from quantum phase transitions at zero temperature in which the energy gap vanishes, the LR Ising models possess another three distinctive regimes with respect to power-law fall-off rate $\alpha$, namely, non-local $(0 < \alpha < 1)$, quasi-local $(1 < \alpha < 2)$ and local $(\alpha > 2)$ according to different scaling law of correlation length [70, 71]. It is important to note here that in the absence of DM interaction, gap-closing never occurs by tuning the parameter $\alpha$ for $h > 0$ except $h_c = 1$. Further, we know that $\alpha \gg 2$, the system with NN interactions becomes gapless for $D > \gamma$ depending on $h$ and the chi-

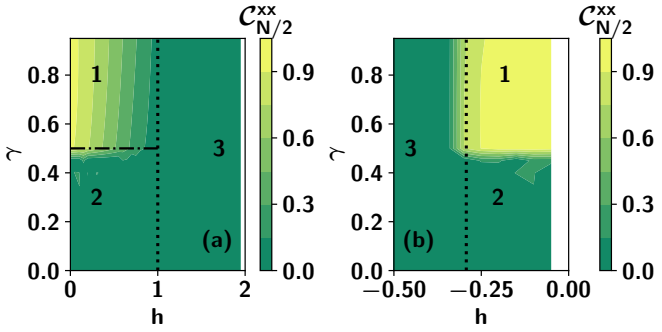


FIG. 2. **Phase diagram of the long-range extended $XY$ model with nonvanishing DM interactions.** Nonvanishing $\mathcal{C}^{xx}_{N/2}$ indicates the $FM_x$ phase for varying external magnetic field, $h$ and the anisotropy parameter, $\gamma$ in the $xy$-plane. For $h > 0$, the critical point is independent of $\alpha$, $FM_x$ extends up to $h = 1$ and bounded by $D = \gamma$ -line in the $y$-direction (see the shaded region Fig (a)). On the other hand, for $h < 0$, critical points depends upon $\alpha$ and $FM_x$ phase is bounded upto $h = -1 + 2^{1-\alpha}$ in the $x$-direction. But the bound in the $y$-direction is not easy to derive which depends non-linearly on $\alpha$ (see the shaded region Fig (b)). Other parameters of the systems are $D = 0.5$, $\alpha = 1.5$ and $N = 512$. All the axis are dimensionless.

ral phase emerges along with paramagnetic and ferromagnetic phases. Due to the long-range DM interactions, a competition between the range of interactions, $\alpha$ and the strength of DM interactions surfaces which becomes responsible for the change in condition for the gapless to gapped transition. More specifically, for moderate values of $\alpha(< 2)$, $D > \gamma$ does not guarantee chiral gapless phase. We find the following in case of LR model.

**Proposition 1.** *For a given value of the magnetic field $h$ (both in $h \geq 0$ and $h < 0$), a gapped to gapless transition occurs when $D > \gamma$ depending upon the value of $\alpha$ instead of $D = \gamma$, known for the NN model.*

*Proof.* The proof is done by analyzing the dispersion relation in Eq. (6). A system is said to be gapped when the expression, $\Delta$ [72, 73], defined as

$$\Delta = \max\{\min\{\epsilon_k\}, 0\} > 0; \quad \forall \phi_k \in [-\pi, \pi], \tag{7}$$

otherwise, the spectrum is gapless (with $\Delta = 0$). The exact point, where the gap-closing takes place, depends on the parameters of the Hamiltonian, and the corresponding momentum, $k_F$, called the Fermi point, can be obtained as a solution of $\frac{\partial \epsilon_k}{\partial k} = 0$. However, due to the presence of long-range order, it is cumbersome to find the Fermi point analytically. By differentiating numerically, we observe that the gapless phase never occurs when $D < \gamma$ while for $D > \gamma$, the gapless phase occurs although it is not ubiquitous, and changes with the variation of $h, D, \gamma$ and $\alpha$. In particular, when $h < 0$, with the decrease of $\alpha$, the system is gapped even when $D > \gamma$ and two distinctive gapped regions emerge when $1 \leq \alpha < 2$ and $0 < \alpha < 1$ which depend on the strength of $D$, thereby inducing (destroying) gapped (gapless) regions. However, for $\alpha > 2$, $D > \gamma$ guarantees gapless phases and the gapless to gapped transition occurs at $D = \gamma$. On the other hand, we find, that when $1 \leq \alpha < 2$, strong DM interactions are required to obtain the gapless phase and the desired asymmetric interaction strength for obtaining the gapless phase *increases* with the decrease of $\alpha$ (see Fig. 1). Note, further, that the maximum $D$ necessary for the gapless phase does not happen exactly at $\alpha = 1$, but at a nearby point which can be due to finite size analysis.

□

It is now evident that the interplay of $\alpha$ and $D$ along with $\gamma$ and $h$ can change the critical lines of the phase diagram. Therefore, we now examine the phases in the $(h, \gamma)$- and $(\alpha, D)$-planes.

*$\alpha$-dependent chiral phase.* In the nearest-neighbor $XY$ model with DM interactions, the gapless phase gives rise to a chiral order that measures local current flow between the nearest neighbor sites. It can be established, by computing [29] the order parameter,

$$\mathcal{CH} = \left\langle \frac{1}{4N} \sum_{i=1}^{N} \sigma_i^x \sigma_{i+1}^y - \sigma_i^y \sigma_{i+1}^x \right\rangle \tag{8}$$

between any two neighboring sites, $i$ and $i+1$ in the ground state which describes the helical alignment of spins or chiral order in the $z$-direction. In the nearest-neighbor case, i.e., for the NN $XY$ model with $D > \gamma$ and suitable $h$ values, it was shown that $\mathcal{CH} > 0$ when $\Delta = 0$.

In the LR model, we find that for a fixed $h$, $\alpha < 2$ and $D > \gamma$, whenever $\Delta = 0$, i.e., the system is gapless, it possesses chiral order with order parameter $\mathcal{CH} > 0$ (as shown in Fig. 1). Interestingly, however, there exists region in which for $D > \gamma$, $\Delta > 0$ (as shown in the above proposition), and the corresponding chiral order parameter vanishes, i.e., $\mathcal{CH} = 0$.

*Ferromagnetic and paramagnetic phases.* We now calculate the long-range magnetic order parameter, $\mathcal{C}^{xx}_{N/2} = \left\langle \sigma_1^x \sigma_{N/2}^x \right\rangle$. When $\mathcal{C}^{xx}_{N/2} \neq 0$, the system is said to be in the ferromagnetic-$x$ phase $(FM_x)$ while paramagnetic when it vanishes. On one hand, we show that the $FM_x$ phase occurs when the system is gapped and $0 < h < h_c^1 = 1$, $1 < \alpha < 2$, and $D < \gamma$ (see Fig. 2). On the other hand, when $h$ is negative, the system becomes ferromagnetic, i.e., $\mathcal{C}^{xx}_{N/2} > 0$ when $h > h_c^2 = -1 + 2^{1-\alpha}$ with $1 < \alpha < 2$. When the parameters are neither chiral nor ferromagnetic, the system is in a paramagnetic phase.

Tuning the strength of the parameters, we can qualitatively describe the phases of this model which changes due to the introduction of long-range interactions. The strength of long-range interactions, $\alpha$, perturbs the system, and can delay the transition from a gapped to a gapless region, although no analytical phase boundary has been established so far. We provide the phase boundaries based on numerical simulations, which depend on $(\alpha)$, $\gamma$, and $h$. More precisely, we present the qualitative phase boundaries for this extended long-range DM model.

1. $D > \gamma$ **and** $\alpha > 2$: The system is in the gapless chiral phase which also depends upon the strength of the

magnetic field $h$, although, the exact boundary is not known.

2. $\forall h,\ D \leq \gamma$ **and** $\alpha > 2$: The system is in the gapped region.

3. $h > 0$ **or** $h < 0$**,** $D > \gamma$ **and** $0 < \alpha < 2$: The system may belong to the gapless chiral region, but depending on the strength of $\alpha$, there exists a gapped region for a fixed $h$, which is an artifact of the long-range interaction strength.

### C. Constant decaying exponent of correlations with DM interactions

From the above analysis, it is evident that the transition from the chiral gapless phase to the other magnetic gapped phase heavily depends on the fall-off rate $\alpha$. Let us now investigate how the scaling of classical correlations and quantum mutual information between two spins (a measure of total correlations containing both quantum and classical correlations components) [74] can recognize the $\alpha$-dependent phases discussed above. The classical correlation (CC) between two sites, separated by a distance $R$, can be represented as $\mathcal{C}_R \equiv \mathcal{C}^{xx}_{i,i+R} = \langle \sigma^x_i \sigma^x_{i+R} \rangle$ while the quantum mutual information is defined as $\mathcal{I}_R \equiv \mathcal{I}_{i:i+R} = S(\rho_i) + S(\rho_{i+R}) - S(\rho_{i,i+R})$, where $S(\sigma) = -\operatorname{tr}(\sigma \log_2 \sigma)$ indicates the von-Neumann entropy of the state $\sigma$, $\rho_i$ and $\rho_{i+R}$ are the reduced density matrices of the joint state $\rho_{i,i+R}$. As we impose periodic boundary condition, the site index $i$ can be ignored and both the classical and total correlation can be studied as $\mathcal{C}^{xx}_R$ and $\mathcal{I}_R$, where $R = \{1, 2, \ldots \frac{N}{2}\}$. In typical one-dimensional (1D) quantum spin models, the CC decays exponentially when it is away from criticality, whereas, at the criticality, the polynomial decay with $R$ is observed. However, the extended Ising model deviates from this norm by showing different scaling laws near the critical points and away from it [75]. Moreover, in the long-range Kitaev chain (see Eq. (3) with $D = 0$), quantum mutual information (QMI) persists between two distant segments of the chain, provided the system is in the non-local regime, i.e., $\alpha < 1$, thereby predicting the correlation between two distant regions of the system [76].

In our study, we expect to have a notable scaling law due to the presence of long-range and additional DM interactions which is indeed the case. Firstly, we observe that the trends of $\mathcal{C}^{xx}_R$ and $\mathcal{I}_R$ with $R$ is qualitatively different when the system is in the chiral phase and when it is not. Secondly, a counter-intuitive observation is that if one tunes the parameters $D$, $\gamma$, $h$ and $\alpha$ in such a way that $\mathcal{CH} \neq 0$, the decay exponents of mutual information and classical correlation become constant as depicted in Fig. 3. Specifically, we observe that irrespective of the details of the power-law exponent and the strength of the magnetic field, the decay exponent of CC and QMI falls off as

$$\mathcal{I}_R \propto R^{-1} \quad \text{and} \tag{9}$$

$$\mathcal{C}^{xx}_R \propto R^{-0.45}, \tag{10}$$

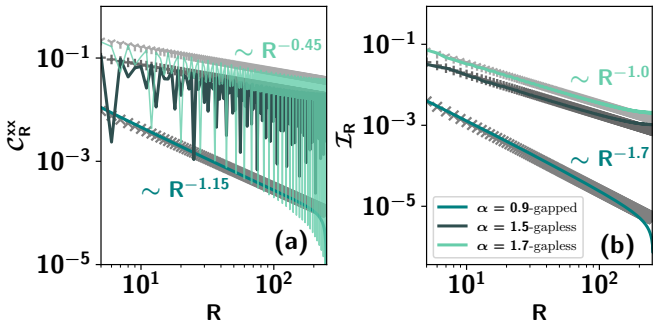


FIG. 3. Classical correlation ($\mathcal{C}^{xx}_R$) and mutual information ($\mathcal{I}_R$) (ordinate) of the bipartite state $\rho_R$ obtained from the ground state vs the distance $R$ (abscissa) between two arbitrary sites, $i$ and $i+R$. The corresponding fit is drawn with a dashed line in the same color. The parameter set of $h = -0.5$ and different values of $\alpha$ indicate whether the system is in a gapless or gapped phase. All other specifications are same as in Fig. 1. All the axes are dimensionless.

which are independent of $\alpha$ provided the ground state belongs to the gapless chiral region (see Fig. 3 and Table I). This behavior of $\mathcal{I}_R$ and $\mathcal{C}^{xx}_R$ highlights a more complex and highly correlated patterns between $\alpha$ and $D$ within the gapless region. It indicates that although the range of interactions can control the critical lines in the $(D, \gamma)$-plane, differentiating gapless and gapped phases, the decay rate of CC and QMI in the gapless phase remains unaltered and the chiral phase favors the sharing of both quantum and classical correlations between distant sites. More importantly, such $\alpha$-dependent scaling behavior holds both for quantum and classical correlations (see Fig. 3).

On the other hand, when the system is in the non-chiral (which we refer to as achiral) phase, the ground state displays the decay exponent of both classical and quantum correlations which vary with $\alpha$, i.e., depending on the internal descriptions of the model (see Fig. 3 and Table I).

Through these observations, we elucidate the nuanced role of long-range DM interactions in modulating correlation properties across both chiral and achiral regions leading to the following proposition.

**Proposition 2.** *In the chiral region of the LR $XY$ model with DM interactions, the scaling exponents of CC and QMI are constant (independent of the fall-off rate, $\alpha$) while their exponents depend on $\alpha$ in the achiral region.*

*Scaling analysis.* To provide insights into the thermodynamic limit, we perform a scaling analysis to understand how the system approaches criticality as the system size increases. Specifically, we analyze $\log_2 |h_c^\infty - h_c^N|$, obtained by computing nearest-neighbor classical correlation $d\mathcal{C}^{xx}_1/dh$, as a function of $\log_2 N$, where $h_c^\infty$ and $h_c^N$ are the critical points in the thermodynamic limit and when the system size is $N$ respectively. The decay of this quantity with $\log_2 N$ indicates that the quantity reaches the thermodynamic limit. Furthermore, the model exhibits critical points at $h_c = 1$ and $h_c = -1 + 2^{1-\alpha}$ for $\alpha > 1$. We demonstrate that the classical correlations in the $x$-direction capture these critical points,

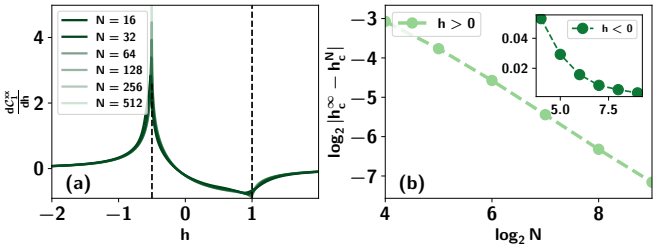


FIG. 4. **Finite size scaling, using nearest-neighbor classical correlation, $\mathcal{C}_1^{xx}$.** (a) A kink in the derivative of $\mathcal{C}_1^{xx}$ indicates the critical points for both $h > 0$ and $h < 0$. For $h > 0$, the critical point is independent of $\alpha$, and the first derivative exhibits a kink at $h_c = 1$, which becomes sharper as the system size $N$ increases. (b) To perform the scaling analysis, we plot $\log_2 |h_c^\infty - h_c^N|$ against $\log_2 N$ where $h_c^\infty = 1$ and $h_c^N$ is the value at which $\mathcal{C}_1^{xx}$ shows the kink for a given system size $N$. Its behavior indicates that $N = 512$ provides a good approximation to the thermodynamic limit. On the other hand, for $h < 0$, the critical point depends on $\alpha$, and is given by $h = -1 + 2^{1-\alpha}$. This critical point exhibits the same trend as the one for $h > 0$, becoming sharper with increasing system size (see the inset of (b)). The system parameters used are $D = 0$ and $\alpha = 2$. All axes are dimensionless.

| D | h | $\alpha$ | $\mathcal{I}_R$ | $\mathcal{C}_R^{xx}$ | Phase |
|---|---|---|---|---|---|
| 1.5 | 0.5 | 0.5 | $R^{-0.25}$ | $R^{-0.3}$ | gapped |
| 1.5 | 0.5 | 0.8 | $R^{-1}$ | $R^{-0.45}$ | gapless |
| 1.5 | 0.5 | 1.3 | $R^{-1}$ | $R^{-0.46}$ | gapless |
| 2.5 | −0.5 | 0.5 | $R^{-0.4}$ | $R^{-0.5}$ | gapped |
| 2.5 | −0.5 | 0.8 | $R^{-1.5}$ | $R^{-1.2}$ | gapped |
| 2.5 | −0.5 | 1.3 | $R^{-1}$ | $R^{-0.45}$ | gapless |

TABLE I. The scaling laws of mutual information $\mathcal{I}_R$ and classical correlation $\mathcal{C}_R^{xx}$ with $R$ for various parameter values of DM interaction strength ($D$), magnetic field ($h$), and power-law exponent ($\alpha$). When the system is gapless, universal scaling exponents for both the quantities emerge which is not the case for the gapped regimes.

and as the system size increases, the identification of these critical points becomes more prominent, as shown in Fig. 4. These results indicate that the classical correlations with system size $N = 512$ indeed mimics the properties with $N \to \infty$ which we again confirm by computing $\mathcal{C}_1^{xx}$ with system size upto $N = 1024$. On the other hand, when calculating the dynamical correlations, we can extend the system size up to $N = 30K$ (see Sec. III). Note, however, it is difficult to provide closed form expressions for the correlators owing to the presence of complicated integrals which is true even for short-range models.

### D. Amendment in scaling of entanglement entropy and central charge owing to long-range DM interactions

In a many-body system, an insight of universality classes can be obtained from the generic features of the ground state. A prominent physical quantity that serves the purpose is the block entanglement entropy of block-size $l$ [77, 78]. In particular, after partitioning the $N$-party ground state into two blocks, containing $l$ and $N-l$ sites (with $l \ll N$), we compute the block entanglement of the ground state as $S_l = S(\rho_l)$ with $\rho_l$ being the reduced density matrix of the $N$-party ground state. The $l$-block entropy can be calculated from the two-point correlation functions between modes, $m$ and $n$, given as

$$C_{mn} = \langle\Psi|c_m^\dagger c_n|\Psi\rangle, \quad F_{mn} = \langle\Psi|c_m^\dagger c_n^\dagger|\Psi\rangle, \tag{11}$$

where $|\Psi\rangle$ is the ground state and the corresponding correlation matrix, consisting of correlation functions, can be written as

$$\mathbb{C}_l = \begin{pmatrix} \mathbb{I} - C & F \\ F^\dagger & C \end{pmatrix}. \tag{12}$$

If $\lambda_p$'s are the eigenvalues of $\mathbb{C}_l$, the von-Neumann entropy of $|\Psi\rangle$ in the bipartition $l : N - l$ is given as $S_l = -\sum_{p=1}^{2l} \lambda_p \log_2 \lambda_p$. If a system is gapped which typically happens away from the criticality and when the range of interactions is relatively local, i.e., the norm of the Hamiltonian does not increase as the system size increases, $S_l$ follows the area law, which implies $S_l^{NC} \propto l^{d-1}$, where $d$ is the spatial dimension of the system and $NC$ stands for "not at criticality" while it deviates from the area law at criticality [78]. Hence from the scaling behavior of $S_l$, one can detect the transition from a gapped to a gapless phase which is interesting since a simple scalar quantity can describe the essential properties of the Hamiltonian instead of a complete microscopic description.

On the other hand, when the system becomes gapless, representing the critical point, e.g., in the transverse NN $XY$ model, $S_l$ scales logarithmically, i.e., for a translationally invariant spin chain, at critical points, $S_l^C = \frac{c}{3}\log_2\left[\frac{N}{\pi}\sin\frac{\pi l}{N}\right] + a$ [78, 79], where $c$ is the *conformal or effective central charge* in the conformal field theory and $a$ is a non-universal constant. Further, it was shown that the central charge carries the signatures of an underlying symmetry. For example, $c$ takes value $1/2$ for the transverse-field Ising-like Hamiltonian at the critical point for which the Hamiltonian adheres to the $\mathbb{Z}_2$-symmetry, while with the addition of asymmetric nearest-neighbor DM interaction, the Hamiltonian becomes gapless region having $c = 1$ and gapped with $c = 1/2$. Hence EE turns out to be a powerful tool to separate a gapped phase from a gapless one.

It was also recently shown that if one considers long-range interactions instead of short-range ones [80, 81], where magnetic criticality depends on the value of $\alpha$, EE depends upon $\alpha$ and the free-fermionic version of long-range Ising spin shows fractal entanglement apart from the volume and area law [64] and the scaling of entropy at critical points may not follow $S_l^C$. In this case, we can define an effective conformal charge, $c_{eff}$, to describe the universal properties of the system.

We are interested in finding how the scaling of $S_l$ in the LR Ising Hamiltonian gets altered in the presence of DM interactions. Specifically, we will show the revision of a central charge $c_{eff}$, which occurs in $S_l^C$. Before presenting the effects of DM interaction on the central charge, we observe that at criticality, i.e., $h_c^1 = 1$ of the extended Ising model, $c_{eff}$

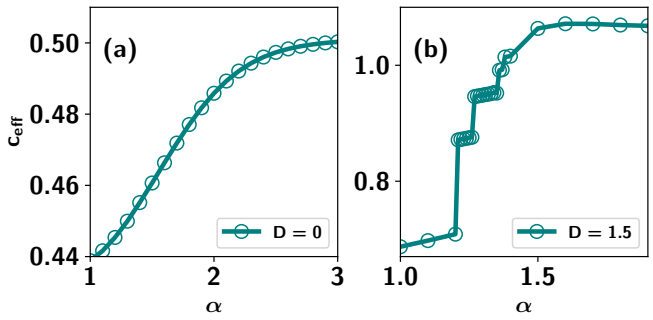


FIG. 5. **Effective central charge, $c_{eff}$ (ordinate) against the the power-law exponent $\alpha$ (abscissa).** We obtain $c_{eff}$ by fitting the block entanglement entropy in the logarithmic scaling equation, $S_l^C = \frac{c_{eff}}{3}\log_2\left[\frac{N}{\pi}\sin\frac{\pi l}{N}\right] + a$ of the ground state at criticality, i.e., $h_c = 1.0$. (a) The non-linear but smooth increase of $c_{eff}$ with $\alpha$ in the absence of asymmetric DM interaction. (b) The abrupt change in $c_{eff}$ against $\alpha$ is observed in the presence of DM interactions for a fixed values of $D$. The kinks possibly arises due to the presence of chirality (gapless). All other specifications are same as in Fig. 1. All the axes are dimensionless.

monotonically increases when $1 < \alpha < 2$ and saturates to $1/2$ at $\alpha \geq 2$, (which is the scaling known for the NN model) as shown in Fig. 5(a). When $\alpha < 2$, $c_{eff}$ varies non-linearly with $\alpha$ which points out that due to the presence of long-range interaction, conformal symmetry breaks down.

On the other hand, the introduction of long-range DM interaction makes more modifications in $c_{eff}$ – (i) the saturation value changes to 1 when $\alpha \to \alpha_c = 2$, with $\alpha_c$ being the point which mimics the NN transverse Ising model with NN DM interactions; (ii) for $\alpha < \alpha_c$, the conformal symmetry breaks down whereas when $\alpha > \alpha_c$, $c_{eff} \to 1$ (see Fig. 5(b)). Our study reveals that even with the introduction of long-range asymmetric interaction, the conformal symmetry is not restored for all the values of $\alpha$ although $c_{eff}$ indicating the conformal invariance begins for smaller values of $\alpha_c < 2$ which is found in the absence of DM interactions. This behavior can again be attributed to the fact that when the DM interaction is present, the system becomes gapless upon varying the power-law decaying factor $\alpha$.

## III. DECAY OF DYNAMICAL CORRELATION: UNCOVERING CHIRAL AND ACHIRAL PHASES

Let us now study the trends of physical quantities including quantum correlations in the time-evolved state in the transient and the steady state regimes, starting from the product state or the ground state which evolves according to the LR Hamiltonian with DM interactions. Our aim is to demonstrate that the scaling of correlations with time or with distant sites can indicate the transition from the chiral phase to the achiral ones.

Note that the NISQ quantum computers are capable of simulating the dynamics of the correlators under scrutiny in this work. A recent study has shown that the truncated Taylor series approach may be used to simulate the dynamics of the correlators [82] while another article [83] describes the realization of a discrete time crystal (DTC) on the Google Sycamore quantum processor. Using a quantum auto-correlator defined as $\langle\sigma^z(0)\sigma^z(n)\rangle$ at the discrete time-steps, $n$ of the associated Floquet drive, the DTC's existence has been verified. The Hamiltonian has been efficiently simulated using the "trotterized" circuit. Therefore, we hypothesize that "trotterization" or truncated Taylor series expansion can be used to examine the dynamics of the correlators in our study in a NISQ computer.

### A. Relaxation behavior of dynamical correlations

Let us first present the method to capture the relaxation of dynamical correlation [54] which is shown to comprehend distinct phases in equilibrium. The initial state and the evolution of the system in the momentum basis can be represented by the Bogoliubov–de Gennes (BdG) equation, given as

$$\psi_k(0) = [u_k(0), v_k(0)]^T \quad \text{and} \quad \psi_k(t) = e^{-iH_k t}\psi_k(0). \tag{13}$$

The corresponding dynamical correlation (DC) is defined as $C_{mn}(t) = \langle\psi(t)|c_m^\dagger c_n|\psi(t)\rangle$ which is a fermionic correlation between two modes. The relaxation of this correlation can be measured by taking the difference between correlation in arbitrary time and time in which the system reaches the steady state, given by $\delta C_{mn}(t) = C_{mn}(t) - C_{mn}(\infty)$, describing the decay of the correlation function with time. Let the Bogoliubov angle of the initial and quenched Hamiltonian be $\eta_k$ and $\tilde{\eta}_k$ respectively and the difference between the angels is given as $\alpha_k = \eta_k - \tilde{\eta}_k$. The relaxation of DC takes the form [84]

$$\delta C_{mn}(t) = \int_{k\in\text{gapped}} \sin 2\tilde{\eta}_k \sin 2\alpha_k \cos(\epsilon_k + \epsilon_{-k})t \cos[k(n-m)] = \tag{14}$$

$$\int_{k\notin\text{gapless}} \sin 2\tilde{\eta}_k \sin 2\alpha_k \cos(\epsilon_k + \epsilon_{-k})t \cos[k(n-m)], \tag{15}$$

where the initial state belongs to the gapped and gapless regions in Eqs. (14) and (15) respectively. In our case, we have chosen $|m-n| = 1$, but our result holds for any arbitrary $m$ and $n$. When $\delta C_{mn}(t) \sim t^{-\chi}$, $\chi$ indicates the dynamical relaxation exponent characterized by the distinctive values of the system parameters.

In the case of the nearest-neighbor $XY$ model, it was shown that the exponent depends on the phase being commensurate or incommensurate. Specifically, in the commensurate phase, the derivative of the dispersion relation with respect to the momentum vanishes at the extreme ends of the Brillouin zone, while in the incommensurate phase, the derivative vanishes inside the Brillouin zone. If the initial state is a product state, i.e., the ground state of the model when the

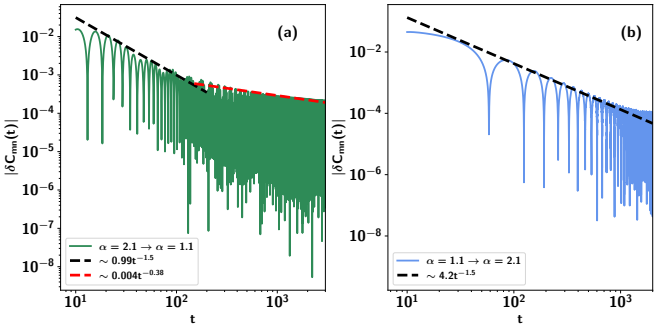


FIG. 6. **The transient dynamics of the $\delta C_{mn}(t)$ (ordinate) as a function of time $t$ (abscissa) in the log-range Ising model with DM interactions**. In both (a) and (b), $h = -0.5, D = 1.3, \gamma = 1.0$, and $N = 30$K for $t = 0$ and for all other values of $t > 0$. For evolution, the sudden quench is performed from $\alpha_i = 2.1$ to $\alpha_q = 1.1$ in (a) and vice-versa in (b). A dashed line is a fit of the function indicating the overall behavior. All the axes are dimensionless.

magnetic field goes to infinity and is then quenched with the Hamiltonian corresponding to the commensurate phase, we find $\chi = 3/2$ while $\chi = 1/2$ when quenched with the incommensurate phase [54].

In the NN $XY$ model with DM interaction, if the initial state belongs to the gapless phase, the exponent changes to $\chi = 1$ if the quenching Hamiltonian is in the commensurate phase, which indicates the presence of DM interaction. In the case of quenching by a Hamiltonian in the incommensurate phase, the exponent is either $\chi = 1/2$ or $\chi = 1$ depending on the parameters of the initial state [84]. On the other hand, considering the LR Kitaev chain, it was found that the scaling law behaves similarly to the SR ones when the initial and post-quench Hamiltonian are non-critical although the exponent changes with the parameters chosen from an equilibrium phase transition [54].

The model considered in this work possesses both LR DM interactions and LR interactions in the $xy$-plane and hence the interplay between $\alpha$ and $D$ as mentioned in the static scenario can influence the scaling of $\delta C_{mn}(t)$, resulting to different $\chi$. For investigations, possible three situations arise in the non-local regime $(\alpha < 1)$ - (ni) both pre- and post-quench Hamiltonian are in the chiral phase; (nii) only pre-quench Hamiltonian belongs to the chiral phase; (niii) only post-quench Hamiltonian is chosen from the chiral phase. All three cases can also be considered when $\alpha$ is chosen from a quasi-local regime, i.e., when $\alpha > 1$ which we refer to as (qi) - (qiii). Eg., we find that $\chi \sim 1.5$ for the case of (niii) and when (qii) $\chi \sim 0.3$ (see Fig. 6). This shows that the exponent in DC can distinguish between the gapped and the gapless phases of the post- and pre-quench Hamiltonians (see Fig. 6). In addition, the robustness of correlation can be defined as a quantity $\frac{1}{\chi}$ such that if the value of $\chi$ is small, the system does not reach the steady state correlation value for a significantly long time. This reinforces the above result that the state from the gapless phase contains a strong correlation both in terms of space and time.

### B. Slow decay of total correlation and two-point correlation with LR DM interaction

We now focus on six scenarios ((ni) - (niii) and (qi) - (qiii)) to study the decay pattern of total correlation and classical correlation with $R$ in a steady state limit, represented by $\mathcal{I}_R(\infty)$ and $\mathcal{C}_R^{xx}(\infty)$ respectively. Even though the evolution is unitary, as we are studying the properties of a subsystem, a steady state can be reached in the dynamics. When the quenching Hamiltonian is in the gapped phase ((nii)), the steady state maintains both classical and quantum correlations between distant spins, and persists even at large distance $R$ (see Figs. 7(b), (c), (f) and (g)). Conversely, a gapless quenching Hamiltonian ((ni) and (niii)) results in a steady state where classical correlations are present only between nearby spins as depicted in Figs. 7 (a), (d), (e) and (h). Notice that the decaying natures of $\mathcal{I}_{\mathcal{R}}(\infty)$ and $\mathcal{C}_R^{xx}(\infty)$ are independent of the initial state. Remarkably, the behavior of total and classical correlations remains similar when the distance between the spins is small.

### C. Effects of long-range in dynamics of EE

In a final attempt to distinguish the gapless and gapped phases under dynamics, we investigate the growth of entropy with time. The initial states are prepared as the ground states of gapped as well as from the gapless regions and EE, $S_l(\rho(t)) \equiv S_t$ for a fixed $l$ is computed after quenching the system to the gapped or gapless regions by changing the parameters $\alpha$ for a given $\gamma, h$ and $D$. Let us denote the initial and final fall-off rates be $\alpha_i$ and $\alpha_q$ respectively. Firstly, we notice that the rate of growth is shown to be linear in time in the case of the $XY$ model with NN [85] and long-range interacting model [86–89], with the initial state being a product state. The trends of $S_t$ with time depend on both $\alpha_i$ and $\alpha_q$, thereby indicating its dependence on pre- and post-quench Hamiltonian. Secondly, the rate of increment of EE with time is faster if the initial state is in a gapless region and the EE value gets saturated around time $t \sim l/2$, as observed in the case of the nearest-neighbor Ising model quenched from a non-critical regime to a critical one [90]. However, if the initial and final states are chosen from a gapless region, the increment rate is slow and the saturation is reached faster around $t = l/2$ compared to a gapped case (see Fig. 8(d) and (e)). Also, the scaling of entropy increment until it reaches saturation can be approximated as

$$S_t^{\pm} \propto a_1 \frac{t}{|\alpha_i \pm \alpha_q|} + a_2, \tag{16}$$

where $a_1$, and $a_2$ are constants (see Fig. 8). When both the initial and the final Hamiltonian are gapped or one of the pre- or post-quench Hamiltonian is gapped, the saturation of EE requires much larger time than that obtained with the Hamiltonians corresponding to the initial and final states being gapless.

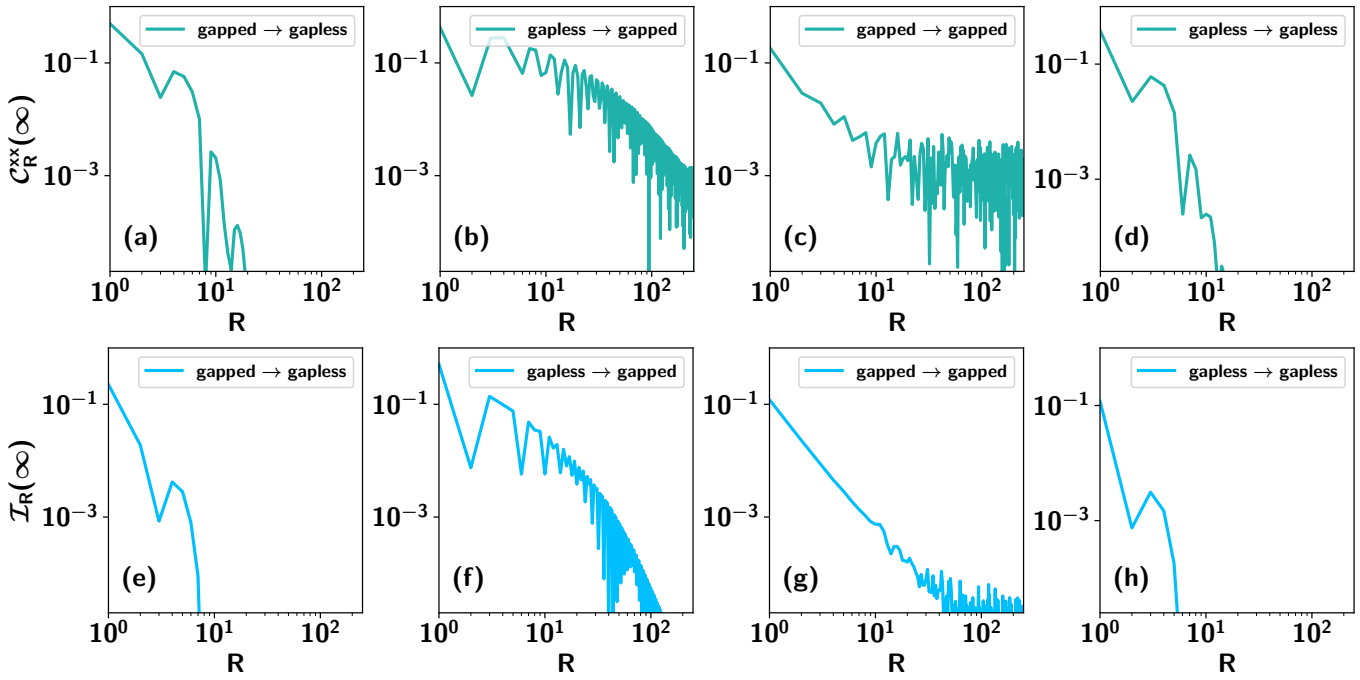


FIG. 7. **Classical and quantum mutual information in the steady state as a function of distance between the spins, $R$ (abscissa) of the LR Ising model with $D = 1.3$.** (a)-(d) Mutual information or total correlation $\mathcal{I}_R(\infty)$ (ordinate) in four different combinations of initial and quenching Hamiltonian picked from the gapped and gapless phases as mentioned in Fig. 6. A similar plot for classical correlation $\mathcal{C}_R^{xx}(\infty)$ in (e)-(f). The strength of the magnetic field $h = -0.5$. Here $N = 512$. Note the striking similarity between the top and bottom rows. All the axes are dimensionless.

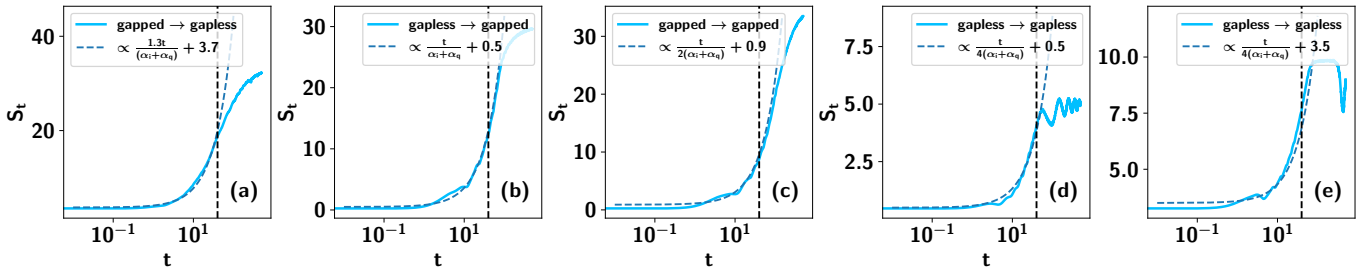


FIG. 8. **Entanglement entropy of block-size $l$ of the quenched state $S_t$ (ordinate) with respect to time $t$ (abscissa).** The parameter sets are given as follows: (a) $h = -0.5, D = 1.3, \alpha_i = 1.1, \alpha_q = 2.1$ that indicates a quenching from a gapped to a gapless phase, (b) $h = -0.5, D = 1.3, \alpha_i = 2.1, \alpha_q = 1.1$ – from a gapless to a gapped quench, (c) $h = -0.5, D = 1.3, \alpha_i = 1.1, \alpha_q = 1.2$ - quenching from a gapped to a gapped phase, (d) $h = -0.5, D = 2.5, \alpha_i = 0.5, \alpha_q = 2.5$ – quenching from a gapless to a gapless phase, and (e) $h = -0.5, D = 2.5, \alpha_i = 2.5, \alpha_q = 0.5$– from a gapless to a gapless quenching. In (d) and (e), a vertical dashed line at $t = \frac{l}{2}$ indicates the saturation time while in (a), (b), (c) saturation does not happen at $t = \frac{l}{2}$ where $l = 80$. In (a), (b), (d), and (e), we present a universal law for the growth of entanglement entropy $S_t^{\pm}$ using a dashed line, mentioned in Eq. (16). All the axes are dimensionless.

## IV. CONCLUSION

Quantum long-range systems are intriguing due to their non-local properties, often displaying counter-intuitive phenomena compared to a short-range Hamiltonian. These models are pervasive in physically realizable systems such as trapped ions and atomic, molecular, and optical setups. Therefore, comprehending their universal features is essential for the advancement of quantum technologies and condensed matter physics.

We found that the long-range extended Dzyaloshinskii-Moriya (DM) interactions with the extended $XY$ model have unique consequences on the critical behavior of the system with a variation of the fall-off rate, $\alpha$, in which the range of interactions between the sites decays. Specifically, even with a comparable or more DM interactions than the anisotropy parameter, we proved that the system remains gapped depending on $\alpha$, which varies with the direction of the transverse magnetic field although the gapless phase still possesses chiral order. By analyzing classical and total correlations between two arbitrary sites of the ground state in the presence of DM inter-

actions, we observed that both of them decay with the distance between the sites and the decay exponent is independent of $\alpha$ in the gapless region while it depends on the system parameters in the gapped regime and decays faster in this case than the gapless zone. Additionally, we exhibited the departures from the universal trend in the block entanglement entropy in presence of long-range DM interactions which could successfully capture the interplay between long-range and DM interactions.

This study investigated how dynamical correlations change in time when the energy spectra of the initial and the evolving Hamiltonian are gapped and gapless, driven by $\alpha$ for a fixed strengths of DM interactions, and magnetic fields. The scaling of both classical correlations and mutual information in the steady states reveals that the sharing of correlations is favorable when the evolving Hamiltonian is gapped. Moreover, we found that the growth of entanglement entropy with time is faster in the gapless regime than in the gapped phase and it saturates quickly when both the pre- and post-quench Hamiltonians are gapless. On the one hand, these findings contribute to the understanding of fundamental aspects of quantum phase transitions, while on the other, sharability of correlations and entanglement of the ground state as well as their dynamical patterns can be vital for establishing quantum links amongst quantum computers.

## ACKNOWLEDGMENTS

We acknowledge the support from the Interdisciplinary Cyber Physical Systems (ICPS) program of the Department of Science and Technology (DST), India, Grant No.: DST/ICPS/QuST/Theme- 1/2019/23. We acknowledge the use of QIClib – a modern C++ library for general purpose quantum information processing and quantum computing (https://titaschanda.github.io/QIClib), numerical computation of Pfaffians by M. Wimmer [91] and the cluster computing facility at the Harish-Chandra Research Institute. This research was supported in part by the "INFOSYS" scholarship for senior students. Funded by the European Union. Views and opinions expressed are however those of the author(s) only and do not necessarily reflect those of the European Union or the European Commission. Neither the European Union nor the granting authority can be held responsible for them. This project has received funding from the European Union's Horizon Europe research and innovation programme under grant agreement No 101080086 NeQST.

[1] O. K. Diessel, S. Diehl, N. Defenu, A. Rosch, and A. Chiocchetta, Generalized higgs mechanism in long-range-interacting quantum systems, Phys. Rev. Res. **5**, 033038 (2023).
[2] N. Defenu, A. Lerose, and S. Pappalardi, Out-of-equilibrium dynamics of quantum many-body systems with long-range interactions, Phys. Rep. **1074**, 1 (2024).
[3] N. Defenu, T. Enss, M. Kastner, and G. Morigi, Dynamical critical scaling of long-range interacting quantum magnets, Phys. Rev. Lett. **121**, 240403 (2018).
[4] N. Defenu, G. Morigi, L. Dell'Anna, and T. Enss, Universal dynamical scaling of long-range topological superconductors, Phys. Rev. B **100**, 184306 (2019).
[5] A. Solfanelli and N. Defenu, Universality in long-range interacting systems: the effective dimension approach (2024), arXiv:2406.14651 [cond-mat.stat-mech].
[6] N. Defenu, D. Mukamel, and S. Ruffo, Ensemble inequivalence in long-range quantum systems (2024), arXiv:2403.06673 [cond-mat.stat-mech].
[7] M. Saffman, T. G. Walker, and K. Mølmer, Quantum information with rydberg atoms, Rev. Mod. Phys. **82**, 2313 (2010).
[8] T. Lahaye, C. Menotti, L. Santos, M. Lewenstein, and T. Pfau, The physics of dipolar bosonic quantum gases, Reports on Progress in Physics **72**, 126401 (2009).
[9] L. D. Carr, D. DeMille, R. V. Krems, and J. Ye, Cold and ultracold molecules: science, technology and applications, New Journal of Physics **11**, 055049 (2009).
[10] R. Blatt and C. F. Roos, Quantum simulations with trapped ions, Nat. Phys. **8**, 277 (2012).
[11] R. Blatt and D. Wineland, Entangled states of trapped atomic ions, Nature **453**, 1008 (2008).
[12] C. Schneider, D. Porras, and T. Schaetz, Experimental quantum simulations of many-body physics with trapped ions, Reports on Progress in Physics **75**, 024401 (2012).
[13] H. Ritsch, P. Domokos, F. Brennecke, and T. Esslinger, Cold atoms in cavity-generated dynamical optical potentials, Rev. Mod. Phys. **85**, 553 (2013).
[14] T. D. Farokh Mivehvar, Francesco Piazza and H. Ritsch, Cavity qed with quantum gases: new paradigms in many-body physics, Advances in Physics **70**, 1 (2021), https://doi.org/10.1080/00018732.2021.1969727.
[15] M. F. Maghrebi, Z.-X. Gong, M. Foss-Feig, and A. V. Gorshkov, Causality and quantum criticality in long-range lattice models, Phys. Rev. B **93**, 125128 (2016).
[16] Z.-X. Gong, M. Foss-Feig, F. G. S. L. Brandão, and A. V. Gorshkov, Entanglement area laws for long-range interacting systems, Phys. Rev. Lett. **119**, 050501 (2017).
[17] Z.-X. Gong, M. F. Maghrebi, A. Hu, M. Foss-Feig, P. Richerme, C. Monroe, and A. V. Gorshkov, Kaleidoscope of quantum phases in a long-range interacting spin-1 chain, Phys. Rev. B **93**, 205115 (2016).
[18] P. Uhrich, N. Defenu, R. Jafari, and J. C. Halimeh, Out-of-equilibrium phase diagram of long-range superconductors, Phys. Rev. B **101**, 245148 (2020).
[19] Monika, L. G. C. Lakkaraju, S. Ghosh, and A. S. De, Better sensing with variable-range interactions (2023), arXiv:2307.06901 [quant-ph].
[20] D. Ghosh, K. D. Agarwal, P. Halder, and A. S. De, Entanglement of weighted graphs uncovers transitions in variable-range interacting models (2023), arXiv:2307.11739 [quant-ph].
[21] I. Dzyaloshinsky, A thermodynamic theory of "weak" ferromagnetism of antiferromagnetics, Journal of Physics and Chemistry of Solids **4**, 241 (1958).
[22] T. Moriya, Anisotropic superexchange interaction and weak ferromagnetism, Phys. Rev. **120**, 91 (1960).
[23] T. Moriya, New mechanism of anisotropic superexchange interaction, Phys. Rev. Lett. **4**, 228 (1960).

[24] D. C. Dender, D. Davidović, D. H. Reich, C. Broholm, K. Lefmann, and G. Aeppli, Magnetic properties of a quasi-one-dimensional s=1/2 antiferromagnet: Copper benzoate, Phys. Rev. B **53**, 2583 (1996).

[25] D. C. Dender, P. R. Hammar, D. H. Reich, C. Broholm, and G. Aeppli, Direct observation of field-induced incommensurate fluctuations in a one-dimensional $S = 1/2$ antiferromagnet, Phys. Rev. Lett. **79**, 1750 (1997).

[26] M. Kohgi, K. Iwasa, J.-M. Mignot, B. Fåk, P. Gegenwart, M. Lang, A. Ochiai, H. Aoki, and T. Suzuki, Staggered field effect on the one-dimensional $S = \frac{1}{2}$ antiferromagnet $\mathrm{yb_4as_3}$, Phys. Rev. Lett. **86**, 2439 (2001).

[27] P. Fulde, B. Schmidt, and P. Thalmeier, Theoretical model for the semi-metal yb4as3, Europhysics Letters **31**, 323 (1995).

[28] S. Stagraczynski, P. Balaz, M. Jafari, J. Barnas, and A. Dyrdal, Magnetic ordering and dynamics in monolayers and bilayers of chromium trihalides: atomistic simulations approach (2024), arXiv:2404.15543 [cond-mat.mes-hall].

[29] R. Jafari, M. Kargarian, A. Langari, and M. Siahatgar, Phase diagram and entanglement of the ising model with dzyaloshinskii-moriya interaction, Phys. Rev. B **78**, 214414 (2008).

[30] Q. Luo, Analytical results for the unusual grüneisen ratio in the quantum ising model with dzyaloshinskii-moriya interaction, Phys. Rev. B **105**, L060401 (2022).

[31] M. Kargarian, R. Jafari, and A. Langari, Dzyaloshinskii-moriya interaction and anisotropy effects on the entanglement of the heisenberg model, Phys. Rev. A **79**, 042319 (2009).

[32] S. Roy, T. Chanda, T. Das, D. Sadhukhan, A. Sen(De), and U. Sen, Phase boundaries in an alternating-field quantum xy model with dzyaloshinskii-moriya interaction: Sustainable entanglement in dynamics, Phys. Rev. B **99**, 064422 (2019).

[33] Z. Ming, X. Hui, L. Xiao-Xian, and T. Pei-Qing, The effects of the Dzyaloshinskii—Moriya interaction on the ground-state properties of the XY chain in a transverse field, Chin. Phys. B **22**, 090313 (2013).

[34] Z.-A. Liu, T.-C. Yi, J.-H. Sun, Y.-L. Dong, and W.-L. You, Lifshitz phase transitions in a one-dimensional gamma model, Phys. Rev. E **102**, 032127 (2020).

[35] R. Houça, A. Belouad, E. B. Choubabi, A. Kamal, and M. El Bouziani, Quantum teleportation via a two-qubit Heisenberg XXX chain with x-component of Dzyaloshinskii–Moriya interaction, J. Magn. Magn. Mater. **563**, 169816 (2022).

[36] H. Wang, G. Wu, and D. Chen, Thermal entangled quantum otto engine based on the two qubits heisenberg model with dzyaloshinskii–moriya interaction in an external magnetic field, Physica Scripta **86**, 015001 (2012).

[37] R. JAFARI and A. LANGARI, Three-qubits ground state and thermal entanglement of anisotropic heisenberg (xxz) and ising models with dzyaloshinskii-moriya interaction, International Journal of Quantum Information **09**, 1057 (2011), https://doi.org/10.1142/S0219749911007800.

[38] E. Mehran, S. Mahdavifar, and R. Jafari, Induced effects of the dzyaloshinskii-moriya interaction on the thermal entanglement in spin-1/2 heisenberg chains, Phys. Rev. A **89**, 042306 (2014).

[39] M. Azimi, L. Chotorlishvili, S. K. Mishra, T. Vekua, W. Hübner, and J. Berakdar, Quantum otto heat engine based on a multiferroic chain working substance, New Journal of Physics **16**, 063018 (2014).

[40] L. Chotorlishvili, M. Azimi, S. Stagraczyński, Z. Toklikishvili, M. Schüler, and J. Berakdar, Superadiabatic quantum heat engine with a multiferroic working medium, Phys. Rev. E **94**, 032116 (2016).

[41] Q. Wang, D. Cao, and H. T. Quan, Effects of the dzyaloshinsky-moriya interaction on nonequilibrium thermodynamics in the $xy$ chain in a transverse field, Phys. Rev. E **98**, 022107 (2018).

[42] M. Azimi, M. Sekania, S. K. Mishra, L. Chotorlishvili, Z. Toklikishvili, and J. Berakdar, Pulse and quench induced dynamical phase transition in a chiral multiferroic spin chain, Phys. Rev. B **94**, 064423 (2016).

[43] T. Farajollahpour and S. A. Jafari, Topological phase transition of the anisotropic $xy$ model with dzyaloshinskii-moriya interaction, Phys. Rev. B **98**, 085136 (2018).

[44] Z.-R. Zhu, Q. Wang, B. Shao, J. Zou, and L.-A. Wu, Effect of the dzyaloshinskii-moriya interaction on quantum speed limit and orthogonality catastrophe, Phys. Rev. A **107**, 042427 (2023).

[45] A. Sen, S. Nandy, and K. Sengupta, Entanglement generation in periodically driven integrable systems: Dynamical phase transitions and steady state, Phys. Rev. B **94**, 214301 (2016).

[46] S. Nandy, K. Sengupta, and A. Sen, Periodically driven integrable systems with long-range pair potentials, Journal of Physics A: Mathematical and Theoretical **51**, 334002 (2018).

[47] M. Sarkar and K. Sengupta, Dynamical transition for a class of integrable models coupled to a bath, Phys. Rev. B **102**, 235154 (2020).

[48] S. Aditya, S. Samanta, A. Sen, K. Sengupta, and D. Sen, Dynamical relaxation of correlators in periodically driven integrable quantum systems, Phys. Rev. B **105**, 104303 (2022).

[49] H. Bernien, S. Schwartz, A. Keesling, H. Levine, A. Omran, H. Pichler, S. Choi, A. S. Zibrov, M. Endres, M. Greiner, V. Vuletić, and M. D. Lukin, Probing many-body dynamics on a 51-atom quantum simulator, Nature **551**, 579 (2017).

[50] G. Delfino and M. Sorba, Persistent oscillations after quantum quenches in d dimensions, Nuclear Physics B **974**, 115643 (2022).

[51] O. A. Castro-Alvaredo, M. Lencsés, I. M. Szécsényi, and J. Viti, Entanglement oscillations near a quantum critical point, Phys. Rev. Lett. **124**, 230601 (2020).

[52] M. Heyl, A. Polkovnikov, and S. Kehrein, Dynamical quantum phase transitions in the transverse-field ising model, Phys. Rev. Lett. **110**, 135704 (2013).

[53] M. Heyl, Dynamical quantum phase transitions: a review, Reports on Progress in Physics **81**, 054001 (2018).

[54] A. A. Makki, S. Bandyopadhyay, S. Maity, and A. Dutta, Dynamical crossover behavior in the relaxation of quenched quantum many-body systems, Phys. Rev. B **105**, 054301 (2022).

[55] F. B. Ramos, A. Urichuk, I. Schneider, and J. Sirker, Power-law decay of correlations after a global quench in the massive xxz chain, Phys. Rev. B **107**, 075138 (2023).

[56] L. G. C. Lakkaraju, S. Ghosh, D. Sadhukhan, and A. S. De, Framework of dynamical transitions from long-range to short-range quantum systems (2023), arXiv:2305.02945 [quant-ph].

[57] D. Sadhukhan, A. Sinha, A. Francuz, J. Stefaniak, M. M. Rams, J. Dziarmaga, and W. H. Zurek, Sonic horizons and causality in phase transition dynamics, Phys. Rev. B **101**, 144429 (2020).

[58] A. Sinha, D. Sadhukhan, M. M. Rams, and J. Dziarmaga, Inhomogeneity induced shortcut to adiabaticity in ising chains with long-range interactions, Phys. Rev. B **102**, 214203 (2020).

[59] M. Kac, G. E. Uhlenbeck, and P. C. Hemmer, On the van der Waals Theory of the Vapor-Liquid Equilibrium. I. Discussion of a One-Dimensional Model, J. Math. Phys. **4**, 216 (1963).

[60] E. Barouch, B. M. McCoy, and M. Dresden, Statistical mechanics of the XY model. i, Phys. Rev. A **2**, 1075 (1970).

[61] E. Barouch and B. M. McCoy, Statistical mechanics of the $xy$ model. ii. spin-correlation functions, Phys. Rev. A **3**, 786 (1971).

[62] E. Lieb, T. Schultz, and D. Mattis, Two soluble models of an antiferromagnetic chain, Annals of Physics **16**, 407 (1961).
[63] G. B. Mbeng, A. Russomanno, and G. E. Santoro, The quantum Ising chain for beginners, SciPost Phys. Lect. Notes , 82 (2024).
[64] A. Solfanelli, S. Ruffo, S. Succi, and N. Defenu, Logarithmic, fractal and volume-law entanglement in a Kitaev chain with long-range hopping and pairing, J. High Energy Phys. **2023** (5), 1.
[65] J. G. Bohnet, B. C. Sawyer, J. W. Britton, M. L. Wall, A. M. Rey, M. Foss-Feig, and J. J. Bollinger, Quantum spin dynamics and entanglement generation with hundreds of trapped ions, Science **352**, 1297 (2016), https://www.science.org/doi/pdf/10.1126/science.aad9958.
[66] S. Hawaldar, P. Shahi, A. L. Carter, A. M. Rey, J. J. Bollinger, and A. Shankar, Bilayer crystals of trapped ions for quantum information processing, Phys. Rev. X **14**, 031030 (2024).
[67] P. Jurcevic, B. P. Lanyon, P. Hauke, *et al.*, Quasiparticle engineering and entanglement propagation in a quantum many-body system, Nature **511**, 202 (2014).
[68] F. Pientka, L. I. Glazman, and F. von Oppen, Topological superconducting phase in helical shiba chains, Phys. Rev. B **88**, 155420 (2013).
[69] E. P. Sinaga, M. P. Adams, E. H. Hasdeo, and A. Michels, Neutron scattering signature of the dzyaloshinskii-moriya interaction in nanoparticles, Phys. Rev. B **110**, 054404 (2024).
[70] D. Vodola, L. Lepori, E. Ercolessi, A. V. Gorshkov, and G. Pupillo, Kitaev chains with long-range pairing, Phys. Rev. Lett. **113**, 156402 (2014).
[71] D. Vodola, L. Lepori, E. Ercolessi, and G. Pupillo, Long-range Ising and Kitaev models: phases, correlations and edge modes, New J. Phys. **18**, 015001 (2015).
[72] M. R. Soltani, F. Khastehdel Fumani, and S. Mahdavifar, Ising in a transverse field with added transverse Dzyaloshinskii-Moriya interaction, J. Magn. Magn. Mater. **476**, 580 (2019).
[73] Q. Luo, Analytical results for the unusual grüneisen ratio in the quantum ising model with dzyaloshinskii-moriya interaction, Phys. Rev. B **105**, L060401 (2022).
[74] B. Groisman, S. Popescu, and A. Winter, Quantum, classical, and total amount of correlations in a quantum state, Phys. Rev. A **72**, 032317 (2005).
[75] D. Sadhukhan and J. Dziarmaga, Is there a correlation length in a model with long-range interactions? (2021), arXiv:2107.02508 [cond-mat.str-el].
[76] G. Francica and L. Dell'Anna, Correlations, long-range entanglement, and dynamics in long-range kitaev chains, Phys. Rev. B **106**, 155126 (2022).
[77] L. Amico, R. Fazio, A. Osterloh, and V. Vedral, Entanglement in many-body systems, Rev. Mod. Phys. **80**, 517 (2008).
[78] P. Calabrese and J. Cardy, Entanglement entropy and quantum field theory, J. Stat. Mech.: Theory Exp. **2004** (06), P06002.
[79] C. Holzhey, F. Larsen, and F. Wilczek, Geometric and renormalized entropy in conformal field theory, Nucl. Phys. B **424**, 443 (1994).
[80] S. Yang, H.-Q. Lin, and X.-J. Yu, Gifts from long-range interaction: Emergent gapless topological behaviors in quantum spin chain (2024), arXiv:2406.01974 [cond-mat.str-el].
[81] D. Chakraborty and N. Angelinos, Entanglement entropy in ground states of long-range fermionic systems (2024), arXiv:2302.06743 [cond-mat.str-el].
[82] J. W. Z. Lau, T. Haug, L. C. Kwek, and K. Bharti, NISQ Algorithm for Hamiltonian simulation via truncated Taylor series, SciPost Phys. **12**, 122 (2022).
[83] M. Ippoliti, K. Kechedzhi, R. Moessner, S. Sondhi, and V. Khemani, Many-body physics in the nisq era: Quantum programming a discrete time crystal, PRX Quantum **2**, 030346 (2021).
[84] K. Cao, Y. Hu, P. Tong, and G. Yang, Dynamical relaxation behavior of an extended xy chain with a gapless phase following a quantum quench, Phys. Rev. B **109**, 024303 (2024).
[85] M. Fagotti and P. Calabrese, Evolution of entanglement entropy following a quantum quench: Analytic results for the $xy$ chain in a transverse magnetic field, Phys. Rev. A **78**, 010306 (2008).
[86] J. Schachenmayer, B. P. Lanyon, C. F. Roos, and A. J. Daley, Entanglement growth in quench dynamics with variable range interactions, Phys. Rev. X **3**, 031015 (2013).
[87] M. Van Regemortel, D. Sels, and M. Wouters, Information propagation and equilibration in long-range kitaev chains, Phys. Rev. A **93**, 032311 (2016).
[88] A. S. Buyskikh, M. Fagotti, J. Schachenmayer, F. Essler, and A. J. Daley, Entanglement growth and correlation spreading with variable-range interactions in spin and fermionic tunneling models, Phys. Rev. A **93**, 053620 (2016).
[89] S. Maity, U. Bhattacharya, and A. Dutta, One-dimensional quantum many body systems with long-range interactions, J. Phys. A: Math. Theor. **53**, 013001 (2019).
[90] P. Calabrese and J. Cardy, Evolution of entanglement entropy in one-dimensional systems, Journal of Statistical Mechanics: Theory and Experiment **2005**, P04010 (2005).
[91] M. Wimmer, Algorithm 923: Efficient Numerical Computation of the Pfaffian for Dense and Banded Skew-Symmetric Matrices, ACM Trans. Math. Softw. **38**, 1 (2012).

## Appendix A: Correlation functions

The two-point correlation functions are the fundamental constituents of our study. In the context of the ground state or the thermal state, the two-site correlation function between sites separated by a distance of $R$ can usually be expressed as a determinant of an $R \times R$ Toeplitz matrix [60–62]. However, as the Hamiltonian includes asymmetric interaction, the bipartite reduced state obtained from the $N$-party ground state after tracing out $N-2$ parties includes the correlators like $\mathcal{C}^{xy} \equiv \langle \sigma_i^x \sigma_{i+R}^y \rangle = \mathrm{tr}(\sigma^x \otimes \sigma^y \rho_R)$ and $\mathcal{C}^{yx}$ along with $\mathcal{C}^{ii}$ $(i = x, y, z)$. Thus for the corresponding density matrix of the two distant parties of the spin chain and the time-evolved state, we need to deal directly with the Pfaffians in order to evaluate the correlations as a function of time as well as distance since there is a formation of chiral phase due to DM interaction.

Using the Pfaffian formalism, we first write the spin correlation functions as

$$\mathcal{C}^{lm}_{i,i+R} = \langle \sigma^l_i \sigma^m_{i+R} \rangle = c(l,m)\mathrm{pf} \begin{vmatrix} I^{lm}_{1,2} & \dots & I^{lm}_{1,R-1} & J^{lm}_1 & F^{lm}_1 & G^{lm}_{1,2} & . & \dots & G^{lm}_{1,r} \\ \dots & \dots & & \dots & \dots & \dots & . & \dots & \dots \\ & & I^{lm}_{R-2,R-1} & J^{lm}_{R-2} & F^{lm}_{R-2} & G^{lm}_{R-2,2} & . & \dots & G^{lm}_{R-2,R} \\ & & & J^{lm}_{R-1} & F^{lm}_{R-1} & G^{lm}_{R-1,2} & . & \dots & G^{lm}_{R-1,R} \\ & & & & E^{lm} & D^{lm}_2 & . & \dots & D^{lm}_R \\ & & & & & K^{lm}_2 & . & \dots & K^{lm}_R \\ & & & & & & H^{lm}_{2,3} & \dots & H^{lm}_{2,R} \\ & & & & & & & \dots & \dots \\ & & & & & & & & H^{lm}_{R-1,R} \end{vmatrix}, \tag{A1}$$

where $c(x,x) = c(y,y) = (-1)^{R(R+1)/2}$,

$$\begin{aligned} I^{xx}_{\mu,\nu} &= \langle A_{l+\mu}(t) A_{l+\nu}(t) \rangle, \\ J^{xx}_{\mu}, &= I^{xx}_{\mu,R}, \\ H^{xx}_{\mu,\nu} &= \langle B_{l+\mu-1}(t) B_{l+\nu-1}(t) \rangle, \\ K^{xx}_{\nu} &= H^{xx}_{1,\nu}, \\ G^{xx}_{\mu,\nu} &= \langle A_{l+\mu}(t) B_{l+\nu-1}(t) \rangle, \\ F^{xx}_{\mu} &= G^{xx}_{\mu,1}, \\ E^{xx} &= G^{xx}_{R,1}, \\ D^{xx}_{\nu} &= G^{xx}_{R,\nu}, \end{aligned} \tag{A2}$$

$$\begin{aligned} I^{yy}_{\mu,\nu} &= \langle A_{l+\mu-1}(t) A_{l+\nu-1}(t) \rangle, \\ J^{yy}_{\mu} &= I^{yy}_{\mu,R}, \\ H^{yy}_{\mu,\nu} &= \langle B_{l+\mu}(t) B_{l+\nu}(t) \rangle, \\ K^{yy}_{\nu} &= H^{yy}_{1,\nu}, \\ G^{yy}_{\mu,\nu} &= \langle A_{l+\mu-1}(t) B_{l+\nu}(t) \rangle, \\ F^{yy}_{\mu} &= G^{yy}_{\mu,1}, \\ E^{yy} &= G^{yy}_{R,1}, \\ D^{yy}_{\nu} &= G^{yy}_{R,\nu}, \end{aligned} \tag{A3}$$

with $s(x,y) = s(y,x) = -i(-1)^{R(R-1)/2}$, we have

$$\begin{aligned} I^{xy}_{\mu,\nu} &= \langle A_{l+\mu}(t) A_{l+\nu}(t) \rangle, \\ G^{xy}_{\mu,\nu} &= \langle A_{l+\mu}(t) B_{l+\nu}(t) \rangle, \\ J^{xy}_{\mu} &= G^{xy}_{\mu,0}, \\ F^{xy}_{\mu} &= G^{xy}_{\mu,1}, \\ H^{xy}_{\mu,\nu} &= \langle B_{l+\mu}(t) B_{l+\nu}(t) \rangle, \\ E^{xy} &= H^{xy}_{0,1}, \\ D^{xy}_{\nu} &= H^{xy}_{0,\nu}, \\ K^{xy}_{\nu} &= H^{xy}_{1,\nu}, \end{aligned} \tag{A4}$$

and

$$\begin{aligned} I^{yx}_{\mu,\nu} &= \langle A_{l+\mu-1}(t) A_{l+\nu-1}(t) \rangle, \\ G^{yx}_{\mu,\nu} &= \langle A_{l+\mu-1}(t) B_{l+\nu-1}(t) \rangle, \\ J^{yx}_{\mu} &= I^{yx}_{\mu,R}, \\ F^{yx}_{\mu} &= I^{yx}_{\mu,R+1}, \\ E^{yx} &= I^{yx}_{r,r+1}, \\ D^{yx}_{\nu} &= G^{yx}_{R,\nu}, \\ K^{yx}_{\nu} &= G^{yx}_{R+1,\nu}, \\ H^{yx}_{\mu,\nu} &= \langle B_{l+\mu-1}(t) B_{l+\nu-1}(t) \rangle. \end{aligned} \tag{A5}$$

Each of the elements in the Pfaffian can be constructed from the expectation values of one of the operators, $A_l A_{l+R}$, $B_l B_{l+R}$ and $A_l B_{l+R}$ with $A_i = c^\dagger_i + c_i, \quad B_i = c^\dagger_i - c_i$.

When recasted in the same Fourier basis as taken while diagonalization, the operators for the $k^{\text{th}}$ momentum have the matrix form

$$(A_l A_{l+R})_k = \begin{bmatrix} \cos(kR) & -i\sin(kR) & 0 & 0 \\ -i\sin(kR) & \cos(kR) & 0 & 0 \\ 0 & 0 & \cos(kR) - i\sin(kR) & 0 \\ 0 & 0 & 0 & \cos(kR) + i\sin(kR) \end{bmatrix}, \tag{A6}$$

$$(B_l B_{l+R})_k = \begin{bmatrix} -\cos(kR) & -i\sin(kR) & 0 & 0 \\ -i\sin(kR) & -\cos(kR) & 0 & 0 \\ 0 & 0 & -\cos(kR) + i\sin(kR) & 0 \\ 0 & 0 & 0 & -\cos(kR) - i\sin(kR) \end{bmatrix}, \tag{A7}$$

$$(A_l B_{l+R})_k = \begin{bmatrix} \cos(kR) & i\sin(kR) & 0 & 0 \\ -i\sin(kR) & -\cos(kR) & 0 & 0 \\ 0 & 0 & 0 & 0 \\ 0 & 0 & 0 & 0 \end{bmatrix}. \tag{A8}$$

The single-site transverse magnetization in the same Fourier basis is given by

$$\sigma_z^k = \begin{bmatrix} -1 & 0 & 0 & 0 \\ 0 & 1 & 0 & 0 \\ 0 & 0 & 0 & 0 \\ 0 & 0 & 0 & 0 \end{bmatrix}. \tag{A9}$$

The corresponding expectation value of the operators for each value of $k$, say $O^k$, with respect to the time-evolved state is computed as $\langle O \rangle = \sum_{k=1}^{N/2} \mathrm{Tr}(\rho_\beta^k(t) O^k)$. Once we find all the single-site magnetizations $m_j^\alpha \ \forall \ \alpha = \{x, y, z\}$ at $j = i$ and $j = i + R$ and all possible two-site correlation functions $\mathcal{C}_{i,i+R}^{l,m} \ \forall \ l, m = \{x, y, z\}$ from the Pfaffians described above, we can construct the two-site reduced density matrix between sites $i$ and $I + R$ as we know any two party density matrix for the given Hamiltonian is given as

$$\rho_{ij} = \frac{1}{4}\left(\mathbb{I}_4 + m^z(\sigma_j^z + \sigma_i^z) + \sum_{k,l} \mathcal{C}_{ij}^{kl} \sigma_i^k \otimes \sigma_j^l\right), \tag{A10}$$

where $k, l \in \{x, y\}$.